Contents lists available at ScienceDirect

Environmental Pollution

journal homepage: www.elsevier.com/locate/envpol

eDNA-based bioassessment of coastal sediments impacted by an oil spill

Yuwei Xie [a], Xiaowei Zhang [a, *], Jianghua Yang [a], Seonjin Kim [b], Seongjin Hong [c], John P. Giesy [a, d, e, f], Un Hyuk Yim [g], Won Joon Shim [g], Hongxia Yu [a], Jong Seong Khim [b, **]

[a] State Key Laboratory of Pollution Control & Resource Reuse, School of the Environment, Nanjing University, Nanjing, 210023, PR China
[b] School of Earth and Environmental Sciences & Research Institute of Oceanography, Seoul National University, Seoul, 08826, Republic of Korea
[c] Department of Ocean Environmental Sciences, Chungnam National University, Daejeon, 34134, Republic of Korea
[d] Department of Veterinary Biomedical Sciences and Toxicology Centre, University of Saskatchewan, Saskatoon, SK, Canada
[e] School of Biological Sciences, University of Hong Kong, Hong Kong, SAR, China
[f] Global Institute for Water Security, University of Saskatchewan, Saskatoon, SK, Canada
[g] Oil and POPs Research Group, Korea Institute of Ocean Science and Technology (KIOST), Geoje, Republic of Korea

ARTICLE INFO

ABSTRACT

Oil spills offshore can cause long-term ecological effects on coastal marine ecosystems. Despite their important ecological roles in the cycling of energy and nutrients in food webs, effects on bacteria, protists or arthropods are often neglected. Environmental DNA (eDNA) metabarcoding was applied to characterize changes in the structure of micro- and macro-biota communities of surface sediments over a 7-year period since the occurrence of *Hebei Spirit* oil *spil*l on December 7, 2007. Alterations in diversities and structures of micro- and macro-biota were observed in the contaminated area where concentrations of polycyclic aromatic hydrocarbons were greater. Successions of bacterial, protists and metazoan communities revealed long-term ecological effects of residual oil. Residual oil dominated the largest cluster of the community-environment association network. Presence of bacterial families (*Aerococcaceae* and *Carnobacteriaceae*) and the protozoan family (*Platyophryidae*) might have conferred sensitivity of communities to oil pollution. Hydrocarbon-degrading bacterial families (*Anaerolinaceae*, *Desulfobacteraceae*, *Helicobacteraceae* and *Piscirickettsiaceae*) and algal family (*Araphid pennate*) were resistant to adverse effects of spilt oil. The protistan family (*Subulatomonas*) and arthropod families (*Folsomia*, *Sarcophagidae Opomyzoidea,* and *Anomura*) appeared to be positively associated with residual oil pollution. eDNA metabarcoding can provide a powerful tool for assessing effects of anthropogenic pollution, such as oil spills on sediment communities and its long-term trends in coastal marine environments.

1. Introduction

Offshore spills of petroleum hydrocarbons, in the form of crude oil, alter structures of coastal ecosystems and thereby cause acute and chronic damages to their functions and services (Peterson et al., 2003; Mendelssohn et al., 2012). Due to its persistence, most of the oil remains in sandy soil of contaminated shorelines, where sedimentary refuges inhibit degradation and sequester persistently toxic oil along the gravel shore (Peterson et al., 2003). Spilled oils can cause various adverse effects on organisms, such as genotoxicity, reproductive toxicity, immunotoxicity, and modulation of endocrine function (Jeong et al., 2015; Ji et al., 2011; Hong et al., 2012, 2014; Barron, 2012; Paul et al., 2013). Spilled oil is often subjected to various physicochemical, biological weathering and degradation processes, and depending on the level of weathering and degradation, compositions of crude oil compounds and its toxicity change with time (Jeong et al., 2015). Effects of more persistent constituents of oil residues can cause long-term population-level effects (Peterson et al., 2003). However, historical assessments of oil spills were limited to short-term monitoring and use of acute toxicity testing of laboratory-tolerant taxa.

Coastal ecosystems can be disturbed by spilt oils due to effects on the bottom of the food chain as well as bioaccumulation, transferring effects of hydrocarbons to higher-trophic-level organisms that can be more visible to and valued by humans (Peterson et al., 2003; Mendelssohn et al., 2012; Silliman et al., 2012). Most current practices for assessment of effects of oil spills focus on monitoring ecological responses of specific communities and/or populations, including microorganisms (King et al., 2015), terrestrial arthropods (Pennings et al., 2014), phytoplankton (Il Lee et al., 2009), zooplankton (McCall and Pennings, 2012), benthic fauna (Seo et al., 2011) and fishes (Jung et al., 2012). Due to the low efficiency of isolation-based morphology approaches, environmental surveys of effects of oil spills on communities of meiofauna cannot consider sufficient numbers of taxa to provide a comprehensive overview. Indirect effects of trophic interactions and interaction cascades can be as significant as direct trophic interactions in structuring ecosystems (Peterson et al., 2003). Despite their key positions in food webs relatively less is known about effects of oil on and recoveries of protists and arthropods (Atlas, 1981). Protists are ubiquitous, unicellular eukaryotes that are essential components of food webs. Protists graze on bacteria and link primary producers and detritivores with higher trophic levels (Clarholm, 1985; Bonkowski and Brandt, 2002; Rocke et al., 2015). Their greater rates of metabolism facilitate fluxes of carbon and energy through ecosystems (Bitencourt et al., 2014). Arthropods can also affect primary production and cycling of nutrients, thus providing valuable linkages and inflows of nutrients that connect disparate parts of ecosystems (Pennings et al., 2014). However, there are literally thousands, if not millions of taxa associated with microbiota, many of which are difficult to identify, classify and enumerate by use of traditional methods of taxonomy.

Environmental DNA (eDNA) metabarcoding provides more powerful tools for monitoring biodiversity in ecosystems (Gibson et al., 2014). eDNA obtained from environmental samples encompasses identification and enumeration of individual taxa that allows fine-scale analyses of ecosystems (Thomsen and Willerslev, 2015), which could allow a more comprehensive characterization of status and trends of communities and during longer-term weathering and recovery of oil spilled in coastal marine ecosystems. Here, we present results of a study that employed semi-quantitative eDNA metabarcoding to assess patterns of successions of bacterial, protistan, and benthic invertebrate communities in intertidal sediments of areas of the Taean coast (South Korea), that were contaminated by the *Hebei Spirit* oil spill (HSOS). The HSOS, which occurred on December 7, 2007, about 10 km off the coast, was the worst oil spill in Korean history. Approximately 10,900 tons of crude oil spread out along a wide stretch of the west coast of Korea. Within one day of the spill, approximately 70 km of the Taean shoreline was visibly contaminated with oil (Hong et al., 2014).

It was hypothesized that the *in situ* micro- and macro-biota could be altered by exposure to crude oil and changes of *in situ* communities (assemblages) could be related to the magnitude of oil pollution. To assess relationships between communities and oil pollution, relative abundances, Shannon diversity, and structure of sedimentary bacterial, protistan, and metazoan communities and abundant assemblages were compared to environmental variables. Diversities and structures of both micro- and macro-biotas were characterized by eDNA metabarcoding (Graphical abstract). This study was focused on sediments from inner parts of semi-closed small bays in the Taean area, where, due to the lack of flushing, relatively great concentrations of crude oil-derived PAHs are still found (Hong et al., 2014).

2. Materials and methods

2.1. Sampling sites and sample collection

A total of 26 surface sediments from heavily contaminated areas (Sinduri dune, Sinduri mudflat, and Sogeunri mudflat) along the Taean coast (Graphical abstract) were used to address long-term community changes over a 7-year period: Specifically, within about one month (December 2007 and January 2008), about one year (June and October 2008), about two years (June 2009), about three years (December 2010), about four years (September 2011 and January 2012), about six years (September 2013) and about seven years (October 2014) after the HSOS (Supplementary Table S1), following previously described sampling procedure (Hong et al., 2012). Four reference sediments were collected from the outer regions of the Taean coast (Naeri) in September 2011. Prior to sampling, residual oil in sediments was visually confirmed at all of the sites. All sediments collected in clean plastic bags were immediately transferred to the laboratory on ice, and then vacuum freeze-dried and stored at −20 °C until analysis.

2.2. Chemical analysis

Total organic carbon (TOC) content of sediments was analyzed using an Elementar Vario Microcube (Hanau, Germany) after removing inorganic carbon by 1M HCl. Concentrations of parent- and alkyl-PAHs were identified and quantified following a previously described method (Hong et al., 2012, 2015a, 2015b). A total of 45 parent- and alkyl-PAHs were measured and summarized in the Supplementary Table S1. To reduce the number of chemical variables, alkyl-PAHs (sum of C1-, C2-, C3- and C4-naphthalen, C1-, C2- and C3-fluorenes, C1-, C2-, C3- and C4-phenanthrenes (Phe), C1-, C2- and C3-dibenzothiophene (Dbthio), C1-, C2- and C3-chrysene (Chr)), parent-PAHs (sum of naphthalene, acenaphthylene, fluorene, Phe, Dbthio, fluoranthene, benz[*a*]anthracene, Chr, benzo[*b*]fluoranthene, benzo[k]fluoranthene, benzo[*a*]pyrene, indeno[1,2,3-*cd*]pyrene, dibenz[ah]anthracene and benzo[ghi]perylene) and total concentration of PAHs (ΣPAHs; sum of alkyl- and parent-PAHs) were used in further analyses. Magnitudes of residual oil weathering in sediments were estimated with alkyl-PAHs double ratios (Hong et al., 2012, 2015a, 2015b; Douglas et al., 1996; Yim et al., 2011). To determine effects of residual oil to communities in sediments, contaminated sediments were grouped according to the magnitude of residual oil pollution; specifically, "greater pollution" group (ΣPAHs $\geq$ 5000 ng/g dry mass (dm)), "lesser pollution" group (ΣPAHs < 5000 and $\geq$ 50 ng/g, dm). Concentrations of ΣPAHs in sediments from the reference site (Naeri) were less than 50 ng/g, dm.

2.3. eDNA extraction, PCR amplification and next-generation sequencing of eDNA

eDNA was extracted from a 0.25 g aliquot of homogenized sediment with the MoBio Power Soil DNA Kit (MoBio Laboratories Inc., CA, USA). Bacterial 16s rRNA genes (V3 fragment), protistan 18s rRNA genes (V9 fragment) and metazoan mitochondria Cytochrome Oxidase subunit I (COI) genes were amplified, purified and sequenced as described previously (Xie et al., 2017; Yang et al., 2017). Ribosomal products were sequenced using an ION proton sequencer (Life Technologies, CA, USA), and the COI products were analyzed with an Ion Torrent PGM sequencer (Life Technologies, CA, USA) according to the manufacturer's instructions.

2.4. Bioinformatics

Raw reads were quality trimmed using the QIIME toolkit (Caporaso et al., 2010). Sequences were only retained if they contained no ambiguous 'N's, a maximum homo-polymer length of eight nucleotides, less than two sample-barcode mismatches and less than four primer mismatches. The reads of V3, V9 and COI were kept if the sequence length was between 130 and 190, 130—170 or 150—400 bp, respectively. Operational taxonomic units (OTUs) for each gene were clustered with a sequence similarity cut-off of 97% following the UPARSE pipeline (Edgar, 2013). Chimeric and singleton OTUs (sizes less than 2) were removed. Bacterial and protistan OTUs were annotated using the RDP classifier (Wang et al., 2007) against the Greengene database (DeSantis et al., 2006) and the protist Ribosomal Reference database (PR2) (Guillou et al., 2013), respectively. The OTUs of COI were annotated using BLAST against the full NCBI nucleotide database returning up to 500 hits per query sequence to determine their probable identities (e-value $\leq$1e-20, percent identity $\geq$ 98%, and word size = 24). Taxonomy was assigned to the best attainable level of taxonomy (generally family or genus) by use of the lowest common ancestor (LCA) algorithm in MEGAN v5.5.3 (default settings except for: min score = 150, top percent = 2) (Huson et al., 2011). Metazoan OTUs were extracted from the whole COI dataset for further analyses. To reduce bias, resulting from in different sequencing depth, OTU tables were rarefied twenty times at equal sequences per sample (bacteria: 21,363; protists: 7982; metazoans: 1220). Richness (observed OTU #) and alpha-diversity (Shannon entropy) were calculated for each rarefaction and then averaged. Beta-diversity was estimated by computing unweighted UniFrac distances (Lozupone and Knight, 2005) between samples from normalized OTU tables using cumulative-sum scaling method (Paulson et al., 2013). Sequence data were deposited into the NCBI Sequence Read Archive under accession number SRS1886231 and SRS1886232.

2.5. Statistics

Statistical analyses were performed using R (http://www.R-project.org/) and PRIMER V7 with PERMANOVA + add-on software (PRIMER-E Ltd, Plymouth, UK). Environmental variables, including ΣPAHs, TOC, latitude and longitude, were log$_{10}$ transformed and normalized. Numbers of months after the HSOS were defined as "Duration". Linear regressions were used to identify significant correlations between pairs of continuous variables. Spearman correlations were used to measure strengths of association between relative abundance and Shannon entropy of taxa and concentration of ΣPAHs. Mantel test was used to assess correlations between concentrations of ΣPAHs and structures of communities (assemblages). Nonmetric multidimensional scaling (NMDS) was used to visualize the levels of dissimilarity of communities. Beta-diversities of communities were compared using permutation-based analyses of variance (PERMAVOVA). The relative contributions of environmental variables in explaining differences in community structures were determined by forward selection distance-based linear modeling (distLM) and distance-based redundancy analyses (dbRDA). The unweighted UniFrac distances of OTU table were used for NMDS, PERMAVOVA, distLM and dbRDA to compare the structure of communities. Euclidean distances of selected environmental variables were used for dbRDA. To identify taxa that might be differentially responsive to magnitudes of residual oils, a univariate test for associations between concentrations of ΣPAHs and the abundant families (mean relative abundance > 0.5%) was conducted by linear discriminant effect size (LEfSe) analysis (Segata et al., 2011). An association network among sedimentary families

was generated by SparCC with 100 bootstraps to assign P-values (Friedman and Alm, 2012). The network was filtered to include only correlations with ρ > 0.50 and a 'two-tailed' P-value < 0.05. Correlations between relative abundance of families and environmental variables were confirmed to be robust if the Pearson's correlation coefficient (|r|) was >0.5 and the adjusted FDR was statistically significant (P$_{FDR}$ < 0.05). The network was displayed and analyzed with Cytoscape V3 (Shannon et al., 2003).

3. Results and discussion

3.1. Descriptions of samples and next-generation sequencing

Since concentrations of ΣPAHs were significantly correlated with concentrations of both parent- and alkyl-PAHs (Pearson correlation, P < 0.05), concentrations of ΣPAHs can be used to characterize both the magnitude of pollution by residual oil and magnitude of weathering of residual oil. Alkyl-PAHs were the major components of oil residue. Geological features of sampling locations along the Taean coast determined distributions of oil from the HSOS. Concentrations of ΣPAHs in heavily contaminated areas had increased since June 2009 (Fig. 1A). Magnitudes of weathering of residual oil in sediments were significantly correlated with concentrations of ΣPAHs (Fig. 1B—D). The half-closed topography of the sampled areas might inhibit wave energy, thus allowing accumulation of residual oils and acting as a sink for recontamination by residual oils. Accordingly the delay in physicochemical degradation and/or sequestered persistently toxic oils could prevail in the intertidal zone of semi-closed coastal areas, especially mud flats (Peterson et al., 2003).

After quality control of raw reads, there were 3,530,567 cleaned, bacterial 16S V3 sequences (74.9% of raw reads; mean sequence length: 162 ± 16 bp), 1,126,907 cleaned, protistan 18S V9 sequences (27.3% of raw reads; mean sequence length: 148 ± 14 bp) and 284,025 cleaned metazoan COI sequences (34.1% raw reads; mean sequence length: 234 ± 98 bp) (Supplementary Table S2). "Dirty" reads due to poor sequencing quality, PCR bias, lack of annotated references or lineage filtering were discarded. In dataset V3, due to low sequencing depth, sample Sogeunri.mf3 was discarded. A total of 11,791 bacterial OTUs, representing 65 bacterial phyla, were discovered. There were 4394 protistan OTUs, representing 26 phyla. For the COI dataset, 2038 metazoan OTUs, representing 14 metazoan phyla, were extracted from the whole COI sequencing dataset (13,396 OTUs). There were three samples (Sinduri.mf8, Sinduri.mf9 and Sogeunri.mf2) discarded due to low depth of sequencing. To capture most of the trends in biodiversities of communities and keep as many samples as possible, bacterial, protistan, and metazoan communities were captured by rarefaction at 21,363, 7,982, and 1220 sequences per sample, respectively, according to the results of rarefaction curves (Supplementary Fig. S1).

3.2. Succession of bacterial communities

Bacterial communities in residual oil-contaminated sediments were significantly different from those of sediments collected from the reference site which indicated that residual oils had altered structures of bacterial communities (Fig. 2; PERMANOVA Pseudo-F = 3.02, P$_{perm}$ value < 0.001). Bacterial communities were dominated by Proteobacteria and Firmicutes (Supplementary Figs. S2 and S3), which is consistent with results of previous studies of oil-contaminated sediments (King et al., 2015; Mason et al., 2014; Rodriguez et al., 2015). Structures of bacterial communities were significantly different among areas with different concentrations of residual oil (Fig. 2A). Structures of bacterial communities in lesser polluted areas were more like those of the reference site than to the
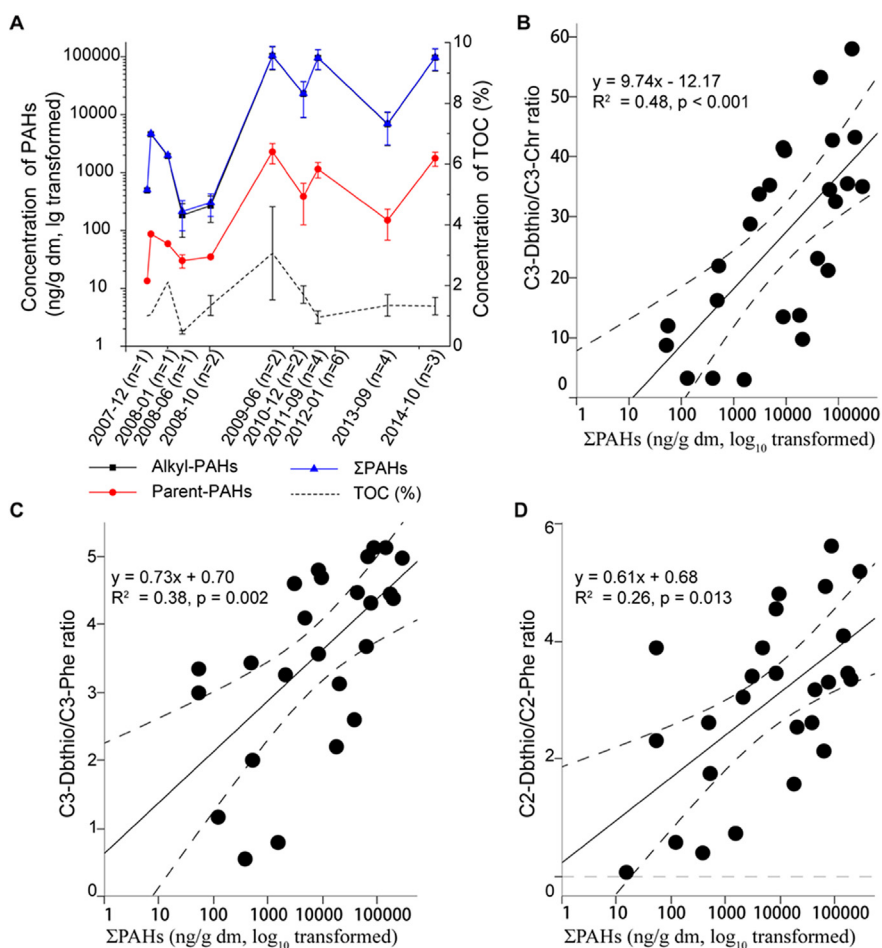
Fig. 1. Temporal changes in chemical characteristics and correlations between indices of oil weathering and concentrations of ΣPAHs in sediments contaminated by the HSOS. (A) Concentrations of TOC, parent- and alkyl-PAHs, and ΣPAHs in sediment collected during various years. Linear regressions between ΣPAHs ($\log_{10}$ transformed) and weathering indices, C3-Dbthio/C3-Chr ratio (B), C3-Dbthio/C3-Phe ratio, and (C), C2-Dbthio/C2-Phe ratio (D).

greater polluted areas (Supplementary Table S3). Furthermore, sedimentary bacterial communities in areas contaminated with greater concentrations of residual oil started diverging from the original status, approximately following temporal changes (Fig. 2B). Patterns of succession of bacterial communities suggested long-term impacts of residual oil pollution on sedimentary bacterial communities.

Among measured environmental variables, structures of bacterial communities were more significantly influenced by residual oil (both duration of exposure to oils and concentrations of ΣPAHs) than Longitude, Latitude or TOC (distLM with unweighted UniFrac distances, Table 1; dbRDA, Fig. 2C). Structures of abundant components of bacterial communities were associated with concentrations of ΣPAHs, except *Verrucomicrobiae* (Supplementary Fig. S4 A). There were significant correlations between concentrations of ΣPAHs and relative abundances of bacterial phyla, including *Firmicutes*, *Proteobacteria* and *Verrucomicrobia* (Supplementary Fig. S4 B and C). At the level of bacterial class, relative abundances of *Bacilli*, *Planctomycetia*, and *Verrucomicrobiae* were negatively correlated with concentrations of ΣPAHs, while relative abundance of ε-*proteobacteria* was positively correlated with concentrations of ΣPAHs. Shannon entropy of δ-*proteobacteria* was positively correlated with concentrations of ΣPAHs, while Shannon entropy of *Verrucomicrobiae* was negatively correlated with concentrations of ΣPAHs. There were six bacterial families associated with magnitudes of residual oil pollution (Fig. 2D). Two *Bacilli* families

(*Aerococcaceae* and *Carnobacteriaceae*) were enriched in sediments less contaminated with oil and negatively correlated with concentrations of ΣPAHs (Fig. 2E and F), while the other four families (*Anaerolinaceae*, *Desulfobacteraceae*, *Helicobacteraceae* and *Piscirickettsiaceae*) were enriched in sediments more contaminated with residual oil (Fig. 2E). Among these tolerant families, relative abundances of *Desulfobacteraceae* and *Anaerolinaceae* were significantly correlated with each other (Pearson correlation, $r > 0.8$, $P < 0.001$) which indicated their coaction in biodegradation of petroleum hydrocarbons at the sites studied.

Shifts of the bacterial communities in sediments contaminated by residual oil could be driven primarily by metabolic activity of degradation and toxic potency of residual oil. Recent metagenomics surveys have repeatedly documented that marine microbiotas in sediments are disturbed by residual oil (King et al., 2015; Mason et al., 2014; Rodriguez et al., 2015). Bacterial communities were reported to be influenced by both direct and indirect pathways due to persistent pollution from oil spills (Peterson et al., 2003). *Aerococcaceae* and *Carnobacteriaceae* were sensitive to effects of residual oils since PAHs and alkyl-PAHs in residual oils can cause general, non-specific effects on the bacterial membrane fluidity due to their accumulation in the lipid bilayer (Camara et al., 2004). Adapted hydrocarbon-degrading populations of microbes can be stimulated to consume certain fractions of petroleum responsible for intrinsic biodegradation (Mason et al., 2014; Kimes et al., 2013). Relative abundances of hydrocarbon-degrading *Proteobacteria* were
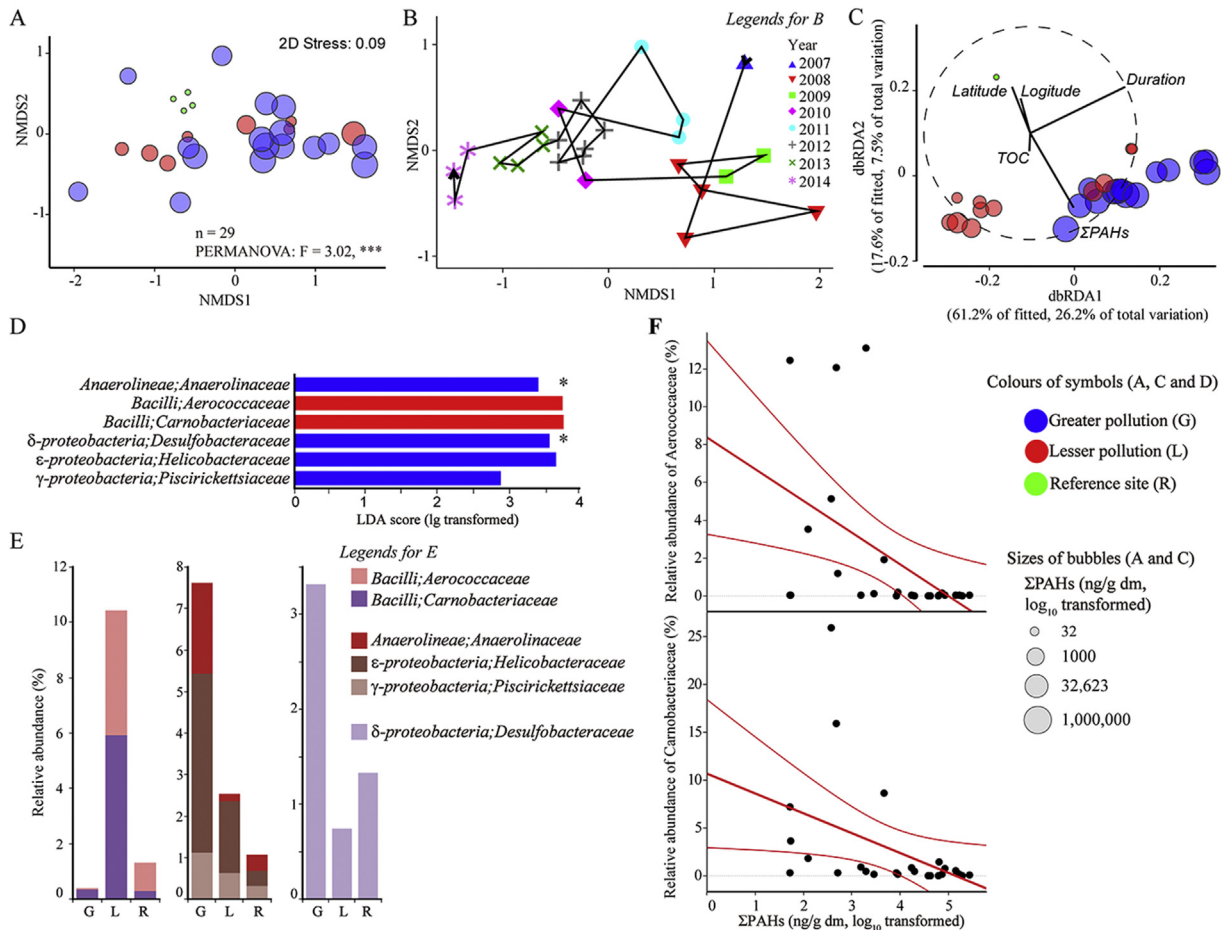
Fig. 2. Succession of sedimentary bacterial communities. (A) Ordination plot of bacterial communities by Non-metric multidimensional scaling (NMDS) with unweighted UniFrac distance. Community-level responses to residual oil pollution were further explored using permutation-based analysis of variance (PERMAVOVA) with unweighted UniFrac distance. P values were calculated using the 9999 permutations procedure. ***: Pperm < 0.001; **: Pperm < 0.01; *: Pperm < 0.05; non-significant (ns): Pperm > 0.05. (B) Temporal succession trajectory of bacterial community structure. (C) Ordination of bacterial community structure by distance-based redundancy analyses (dbRDA) in relation to environmental variables. (D) Association of abundant bacterial families with magnitudes of residual oil pollution by linear discriminant effect size (LEfSe) analyses. Families with a log-transformed linear discriminant analysis (LDA) score > 3 are plotted. *, highly correlated subgroup (Pearson correlation coefficient > 0.8). (E) Significantly different bacterial families among magnitudes of residual oil pollution (Kruskall-Wallis tests, P-values < 0.05). (F) Linear regression of the relative abundance of bacterial families to concentrations of ΣPAHs. Samples from reference site were excluded. Families with P-values < 0.05 are plotted. ΣPAHs was $\log_{10}$ transformed.

Table 1
DistLM results of community structures against measured environmental variables in the full analysis (9999 permutations). Concentrations of ΣPAHs were $\log_{10}$ transformed.

| Community	Variable	Marginal tests		Sequential tests		
		Pseudo-F	Prop.[a]	Pseudo-F	Prop.[a]	Cumul.[b]
Bacteria	Duration	**7.86**	**22.5**	**7.86**	**22.5**	**22.5**
	ΣPAHs	**4.43**	**14.1**	**3.47**	**9.1**	**31.6**
	Longitude	**3.46**	**11.4**	**2.09**	**5.3**	**36.9**
	Latitude	**2.68**	**9.0**	1.12	2.8	39.7
	TOC	1.21	4.3	1.22	3.0	42.7
Protists	Duration	**2.68**	**8.7**	**2.68**	**8.7**	**8.7**
	ΣPAHs	**2.66**	**8.7**	**2.18**	**6.8**	**15.5**
	Longitude	**2.55**	**8.4**	1.52	4.7	20.2
	Latitude	**2.04**	**6.8**	0.94	2.9	23.1
	TOC	1.26	4.3	1.45	4.4	27.5
Metazoans	Duration	**6.14**	**19.7**	**6.14**	**19.7**	**19.7**
	ΣPAHs	**2.78**	**10.0**	1.76	5.5	25.2
	Longitude	**2.46**	**9.0**	1.82	5.5	30.7
	Latitude	1.59	6.0	0.79	2.4	33.1
	TOC	0.81	3.1	1.28	3.8	36.9

[a] Prop.: Percentage of variation explained (%).
[b] Cumul.: Cumulative percentage of variation explained (%). Bold = significantly correlated with community structure at a <0.05.

resistant to effects of residual oil and their populations were simulated by oil in sediments (Gieg et al., 2014). Previously described hydrocarbon-degrading bacteria, including *Piscirickettsiaceae*, sulfate-reducing *Desulfobacteraceae* and *Helicobacteraceae, and* secondary degraders *Anaerolinaceae*, were enriched in sediments contaminated by residual oil (Kleinsteuber et al., 2012; Suarez-Suarez et al., 2011; Hawley et al., 2014; Rivers et al., 2013; Bargiela et al., 2015; Dubinsky et al., 2013).

3.3. Succession of protistan communities

Protistan communities in sediments contaminated by residual oil were significantly different from that of the reference site, which revealed that residual oil had altered structures of protistan communities (Fig. 3; PERMANOVA Pseudo-F = 2.04, Pperm value < 0.001). Coastal benthic habitats harbored a significant diversity of microscopic eukaryotic taxa, including algae, fungi and protozoa. Predominant protistan super-groups in the residual oil-contaminated sediments included *Alveolata, Stramenopiles, Rhizaria, Archeaepplastida* and *Opisthokonta* (Supplementary Figs. S2 and S3). Like the results of molecular surveys of protistan biodiversity in European coastal sediments (Massana et al., 2015), algal
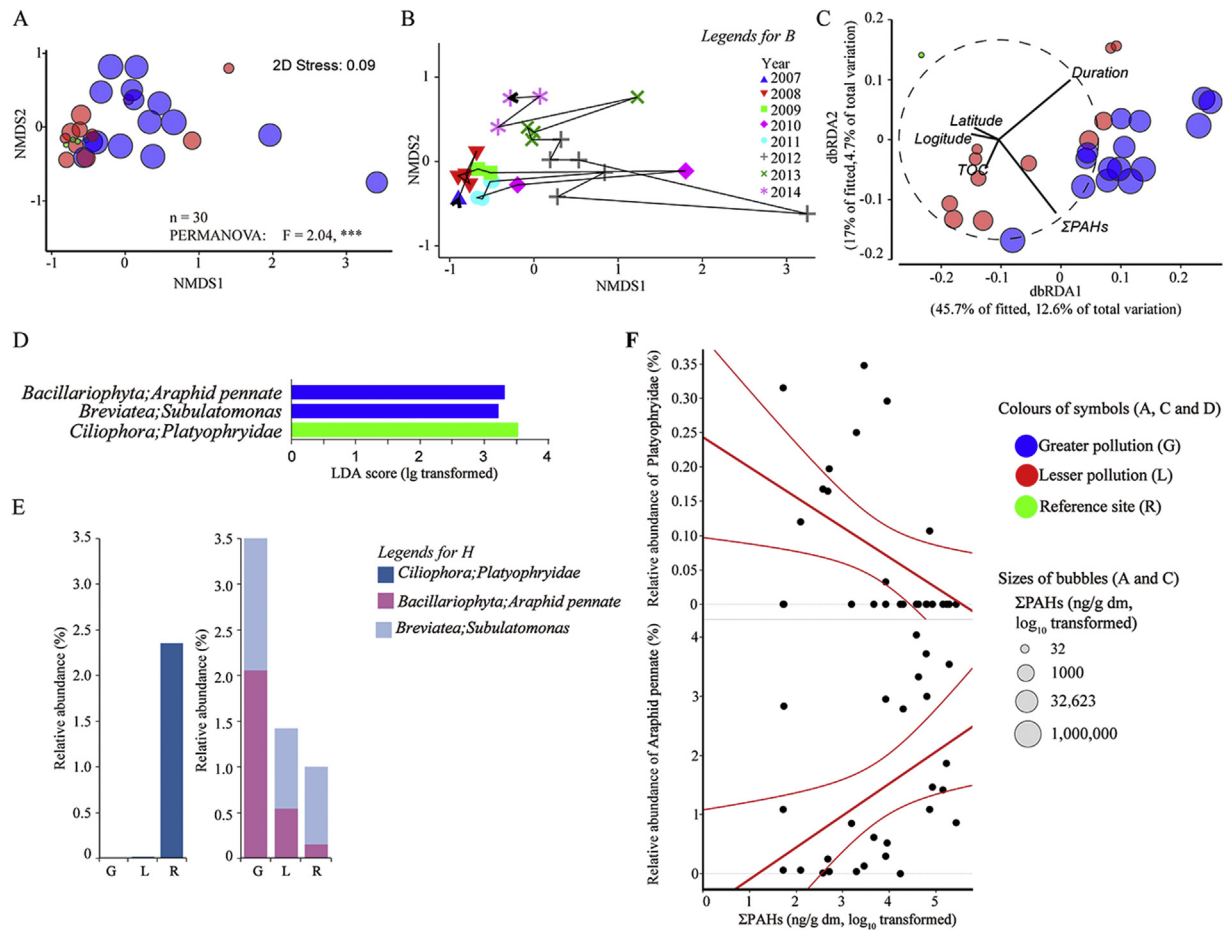
Fig. 3. Succession of sedimentary protistan communities. (A) Ordination plot of protistan communities by NMDS with unweighted UniFrac distance. Community-level responses to residual oil pollution were further explored using PERMAVOVA with unweighted UniFrac distance. P values were calculated using the 9999 permutations procedure. ***: Pperm < 0.001; **: Pperm < 0.01; *: Pperm < 0.05; non-significant (ns): Pperm > 0.05. (B) Temporal succession trajectory of protistan community structure. (C) Ordination of protistan community structure by dbRDA in relation to environmental variables. (D) Association of abundant protistan families with magnitudes of residual oil pollution by LEfSe analyses. Families with a log-transformed linear discriminant analysis (LDA) score > 3 are plotted. (E) Significantly different protistan families among magnitudes of residual oil pollution (Kruskall-Wallis tests, P-values < 0.05). (F) Linear regression of the relative abundance of protistan families to concentrations of ΣPAHs. Samples from reference site were excluded. Families with P-values < 0.05 are plotted. ΣPAHs was log₁₀ transformed.

communities were dominated by *Chlorophyta*, *Dinophyta*, and *Ochrophyta*, while protozoan communities were dominated by *Apicomplexa*, *Cercozoa* and *Cliliophora*. Structures of protistan communities were significantly different among areas with various magnitudes of contamination with residual oil (Fig. 3A). Structures of protistan communities in areas less contaminated with residual oil were more similar to more contaminated areas than they were to the reference site (Supplementary Table S3). Also, protistan communities in sediments where concentrations of residual oil remained relatively constant from 2007 to 2011, and started diverging from the original status, approximately following trajectories observed for 2012, 2013 and 2014 (Fig. 3B).

Changes in structures of protistan communities were mostly associated with concentrations of ΣPAHs among measured environmental variables (Table 1 and Fig. 3C). Structures of algal communities were associated with magnitudes of residual oils (Supplementary Fig. S4 A). Among algae, the relative abundance of *Bacillariophyta* and Shannon entropy of Chlorophyta were positively correlated with concentrations of ΣPAHs (Supplementary Fig. S4 B and C). Shannon entropy of protozoan assemblages was significantly correlated with concentrations of ΣPAHs (Supplementary Fig. S4 A). Almost all abundant components of protozoan assemblages were associated with concentrations of

ΣPAHs *via* changes of relative abundance, diversity, or structure (Supplementary Fig. S4). *Araphid pennate* (diatom) and *Subulatomonas* (*Breviatea*) were enriched in sediments where concentrations of oil were greater, while *Platyophryidae* (ciliate) was enriched in sediments at the reference site (Fig. 3D and E). Also, relative abundances of *Platyophryidae* were negatively associated with concentrations of ΣPAHs, while relative abundances of *Araphid pennate* were positively associated with concentrations of ΣPAHs (Fig. 3E and F).

Despite potential contributions of unmeasured environmental variables, concentrations of residual oil drove changes in protistan communities in sediments. Based on negative associations with magnitude of residual oils, protistan communities and assemblages of protists (*Ciliophora*, *Apusomonadidae*, and *Cercozoa*) were sensitive to effects of residual oils due to direct and/or indirect toxic effects (Almeda et al., 2014; Enrique et al., 2007; Cerezo and Agusti, 2015). Relative abundances of another little-known free-living ciliate, *Platyophryidae*, were negatively associated with residual oil pollution, potentially due to multiple toxic effects of both PAHs and alkyl-PAHs (Bamforth and Singleton, 2005). *Araphid pennate* was tolerant to toxicity of residual oils and able to biodegrade oil (Chan et al., 2006). A population of tolerant microbial predators might be stimulated due to increasing food supply. The relative abundance of

Subulatomonas was positively associated with magnitude of residual oils, which could inhibit degradation of hydrocarbon through predation on protists or bacteria that might degrade hydrocarbons (Kobayashi et al., 2013). Communities of protists were significantly correlated with both bacterial and metazoan communities in sediments contaminated by residual oil (Mantel test: Rho = 0.790, P-value < 0.001), which indicated that protists serve as a bridge from primary producers to higher trophic level organisms. Hence, toxic fractions of petroleum can affect upper trophic level organisms through food chains (Clarholm, 1985; Bonkowski and Brandt, 2002; Rocke et al., 2015).
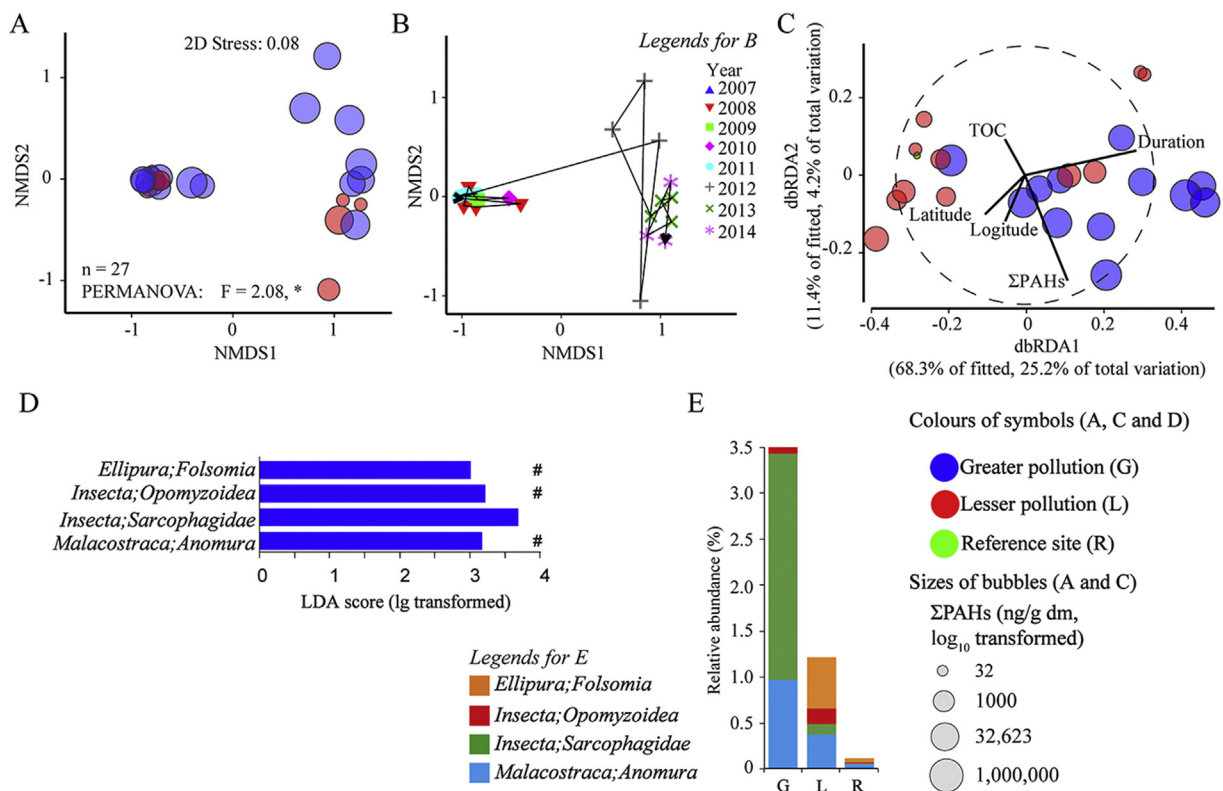
3.4. Succession of metazoan communities

Metazoan communities in sediments contaminated by residual oil were significantly different from that of the reference sediment (Fig. 4; PERMANOVA Pseudo-F = 2.08, P_{perm} value < 0.05). *Insecta* dominated metazoan communities in sediments more contaminated with residual oils (Supplementary Figs. S2 and S3). Structures of metazoan communities displayed a significant separation among sediments with varying concentrations of residual oil (Fig. 4A). Metazoan communities in sediments where concentrations of residual oil were greater were relatively stable from 2007 to 2011, but changes/in 2012 (Fig. 4B). Structures of metazoan communities in lesser contaminated sediments were more like those at the reference site than they were to those at more contaminated sediments (Supplementary Table S3). Shannon entropy and structures of metazoan communities were significantly associated with concentrations of ΣPAHs (Supplementary Fig. S4 A).

Variations in communities of metazoans were associated with concentrations of ΣPAHs, which revealed pressures of residual oils on metazoan communities in sediments more contaminated with residual oil (Table 1 and Fig. 4C). Relative abundances of almost all assemblages of metazoans, except *Arachnida*, were significantly correlated with concentrations of ΣPAHs (Supplementary Fig. S4 B). *Folsomia* (*Ellipura*), *Opomyzoidea* (*Insecta*), *Sarcophagidae* (*Insecta*) and Anomura (*Malacostraca*) were enriched in sediments more contaminated with oil. Relative abundances of *Folsomia*, *Opomyzoidea* and *Anomura* were significantly correlated with each other (Pearson correlation, r > 0.8, P value < 0.001) (Fig. 4D and E).

Metazoan communities in sediments more contaminated with residual oils were driven by both direct and indirect effects of residual oils (Peterson et al., 2003). In general, four arthropod families, *Folsomia*, *Opomyzoidea*, *Sarcophagidae*, and *Anomura*, were more tolerant of effects of oil. Their tolerances of residual oils were consistent with results of more potent toxicity tests. Increasing relative abundance of springtail (*Folsomia*) might be due to elimination of fractions of ΣPAHs of lesser mass (Turner et al., 2014). The maximum concentration of ΣPAHs (271 mg/kg, dm sediment) was less than the reported EC50, based on reproduction of *Folsomia candida* (2662 mg oil/kg, dm soil) (van Gestel et al., 2001). Red king crab (*Anomura*) can survive in water contaminated with 5.4 mg ΣPAHs/L (Sagerup et al., 2016), while the maximum concentration of parent PAHs was 3.54 mg/kg, dm sediment. Since there are few studies of toxic effects of oil on *Opomyzoidea* or *Sarcophagidae*, reasons, why their relative abundances, increased were not clear.

Fig. 4. Succession of sedimentary metazoan communities. (A) Ordination plot of metazoan communities by NMDS with unweighted UniFrac distance. Community-level responses to residual oil pollution were further explored using PERMAVOVA with unweighted UniFrac distance. P values were calculated using the 9999 permutations procedure. ***: Pperm < 0.001; **: Pperm < 0.01; *: Pperm < 0.05; non-significant (ns): Pperm > 0.05. (B) Temporal succession trajectory of metazoan community structure. (C) Ordination of metazoan community structure by dbRDA in relation to environmental variables. (D) Association of abundant metazoan families with magnitudes of residual oil pollution by LEfSe analyses. Families with a log transformed linear discriminant analysis (LDA) score > 3 are plotted. #, highly correlated subgroup ($|r_{Pearson}| > 0.8$). (E) Significantly different metazoan families among magnitudes of residual oil pollution (Kruskall-Wallis tests, P-values < 0.05).

Alternatively, greater relative abundances of these families of arthropods might be due to absence or at least much reduced relative abundances of other more sensitive populations.

3.5. Sedimentary community-environment association network

The eDNA-based sedimentary community-environment association network integrating data on bacterial, protists, metazoan community and environmental variables, revealed effects of residual oil pollution and spatial factors, as well as temporal changes in compositions of communities. The resulting association network consisted of 194 edges (significant correlations, P value < 0.05) among 120 nodes (115 families and 5 environmental variables) (Fig. 5). Five clusters were identified in the association network. Cluster I placed protists associated with residual oil pollution as a central hub in sedimentary communities. Clusters II and III circumscribed spatio-temporal variability in benthic communities. Cluster IV represented cross-trophic relationships and linked Cluster I, II, III and V through both direct and indirect correlations.

The sedimentary community-environment association network highlighted systematic effects of residual oil pollution on sedimentary bacterial, protistan and metazoan communities.

Consistent with results of LEfSe, the ΣPAHs, the dominant node in Cluster I, was positively correlated with numbers of oil-degrading related micro taxa. For instance, hydrocarbon-degrading taxa (*Araphid pennat* (Chan et al., 2006)), sulfate reducer (*Desulfobacteraceae* (Suarez-Suarez et al., 2011) *and Deferribacteraceae* (Orphan et al., 2000)), anaerobic halogenated hydrocarbons degrader (*Dehalobacteriaceae* (Maillard et al., 2003)) and secondary degraders (*Anaerolinaceae* (Kleinsteuber et al., 2012)). Negative correlations in Cluster I revealed toxic effects of residual oils resulting mainly from PAHs (Hong et al., 2012). Due to persistence of the residual oils, contamination by residual oil, coupled with spatial and temporal factors, influenced communities in sediments or areas more contaminated with residual oil through relationships across multiple trophic levels (Peterson et al., 2003).

4. Conclusions

The study investigated biodiversity of micro- and macro-biotas by eDNA metabarcoding and assessed their associations with residual oil pollution of sediments more than eight years after the HSOS. The residual oil pollution caused the Changes in communities of micro and macro-biotas were associated with residual oil
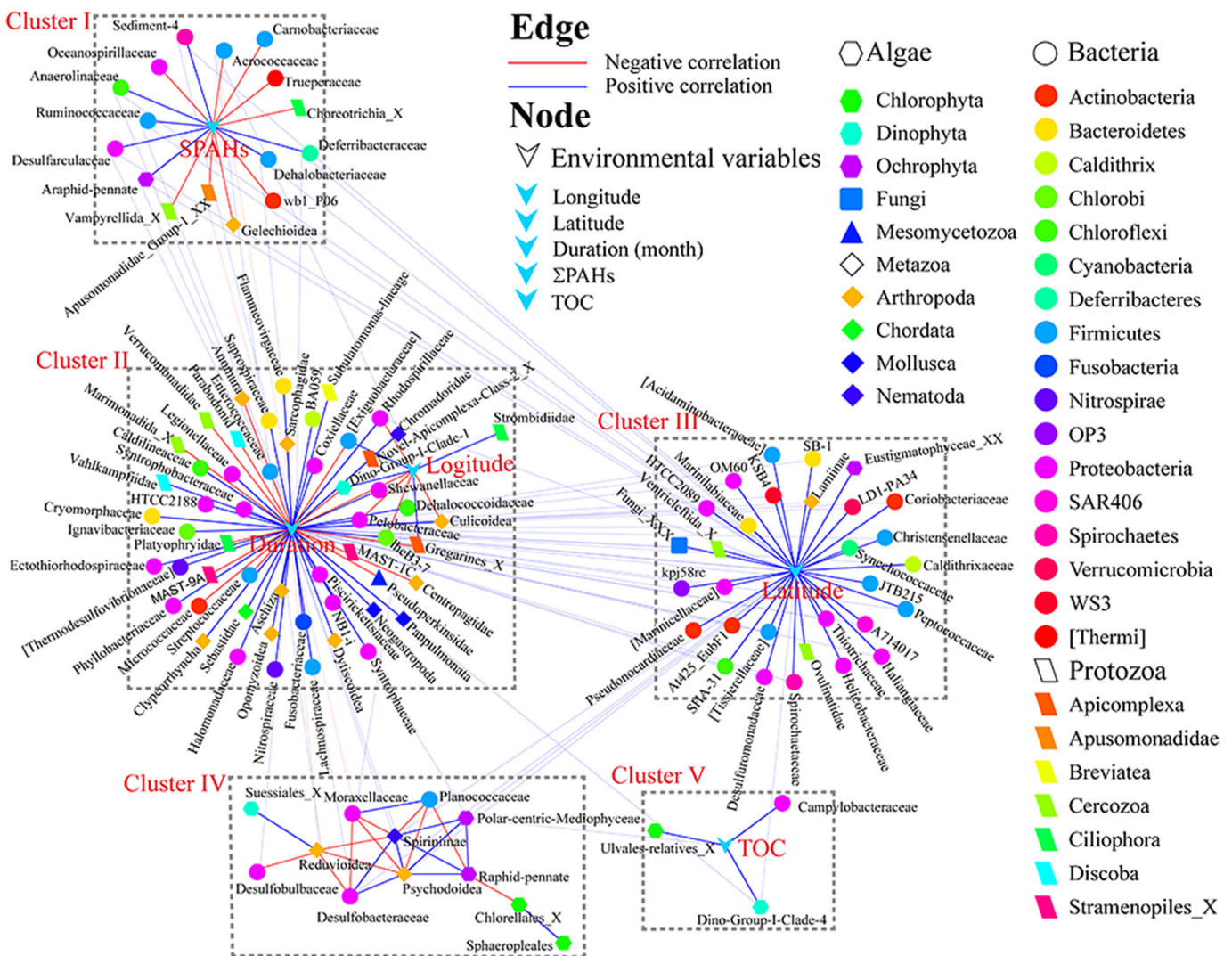

Fig. 5. Plot of sedimentary community-environment association network. Correlation coefficients between two nodes were labelled, the positive coefficient in red, while negative coefficient in blue. (For interpretation of the references to colour in this figure legend, the reader is referred to the Web version of this article.)

pollution. Shannon entropy and structures among multiple communities as a function of ΣPAHs demonstrated that the residual oil pollution was the primary factor regulating dynamics of community structures. Besides the natural spatial-temporal changes, the succession of bacterial, protistan and metazoan communities was driven by the long-term effects of residual oil pollution from HSOS. eDNA metabarcoding is one informative, comprehensive and cost-effective method for long-term biomonitoring. Couple with traditional biomonitoring techniques, eDNA metabarcoding could be used for assessment of environmental quality and ecosystem health.

Acknowledgments

Appendix A. Supplementary data

Supplementary data related to this article can be found at https://doi.org/10.1016/j.envpol.2018.02.081.

References

Almeda, R., Hyatt, C., Buskey, E.J., 2014. Toxicity of dispersant Corexit 9500A and crude oil to marine microzooplankton. Ecotoxicol. Environ. Saf. 106, 76–85.

Atlas, R.M., 1981. Microbial-degradation of petroleum-hydrocarbons - an environmental perspective. Microbial. Rev. 45 (1), 180–209.

Bamforth, S.M., Singleton, I., 2005. Bioremediation of polycyclic aromatic hydrocarbons: current knowledge and future directions. J. Chem. Technol. Biotechnol. 80 (7), 723–736.

Bargiela, R., Gertler, C., Magagnini, M., Mapelli, F., Chen, J., Daffonchio, D., Golyshin, P.N., Ferrer, M., 2015. Degradation network reconstruction in uric acid and ammonium amendments in oil-degrading marine microcosms guided by metagenomic data. Front. Microbiol. 6, 1270–1275.

Barron, M.G., 2012. Ecological impacts of the Deepwater Horizon oil spill: implications for immunotoxicity. Toxicol. Pathol. 40 (2), 315–320.

Bitencourt, J.A.P., Silva, F.S., da Silva-Neto, I.D., Crapez, M.A.C., 2014. Protists and bacteria interactions in the presence of oil. An. Acad. Bras. Cienc. 86 (2), 745–754.

Bonkowski, M., Brandt, F., 2002. Do soil protozoa enhance plant growth by hormonal effects? Soil Biol. Biochem. 34 (11), 1709–1715.

Camara, B., Herrera, C., Gonzalez, M., Couve, E., Hofer, B., Seeger, M., 2004. From PCBs to highly toxic metabolites by the biphenyl pathway. Environ. Microbiol. 6 (8), 842–850.

Caporaso, J.G., Kuczynski, J., Stombaugh, J., Bittinger, K., Bushman, F.D., Costello, E.K., Fierer, N., Pena, A.G., Goodrich, J.K., Gordon, J.I., Huttley, G.A., Kelley, S.T., Knights, D., Koenig, J.E., Ley, R.E., Lozupone, C.A., McDonald, D., Muegge, B.D., Pirrung, M., Reeder, J., Sevinsky, J.R., Tumbaugh, P.J., Walters, W.A., Widmann, J., Yatsunenko, T., Zaneveld, J., Knight, R., 2010. QIIME allows analysis of high-throughput community sequencing data. Nat. Meth. 7 (5), 335–336.

Cerezo, M.I., Agusti, S., 2015. Polycyclic aromatic hydrocarbons alter the structure of oceanic and oligotrophic microbial food webs. Mar. Pollut. Bull. 101 (2), 726–735.

Chan, S.M., Luan, T., Wong, M.H., Tam, N.F., 2006. Removal and biodegradation of polycyclic aromatic hydrocarbons by Selenastrum capricornutum. Environ.

Toxicol. Chem./SETAC 25 (7), 1772–1779.

Clarholm, M., 1985. Interactions of bacteria, protozoa and plants leading to mineralization of soil-nitrogen. Soil Biol. Biochem. 17 (2), 181–187.

DeSantis, T.Z., Hugenholtz, P., Larsen, N., Rojas, M., Brodie, E.L., Keller, K., Huber, T., Dalevi, D., Hu, P., Andersen, G.L., 2006. Greengenes, a chimera-checked 16S rRNA gene database and workbench compatible with ARB. Appl. Environ. Microbiol. 72 (7), 5069–5072.

Douglas, G.S., Bence, A.E., Prince, R.C., McMillen, S.J., Butler, E.L., 1996. Environmental stability of selected petroleum hydrocarbon source and weathering ratios. Environ. Sci. Technol. 30 (7), 2332–2339.

Dubinsky, E.A., Conrad, M.E., Chakraborty, R., Bill, M., Borglin, S.E., Hollibaugh, J.T., Mason, O.U., Y, M.P., Reid, F.C., Stringfellow, W.T., Tom, L.M., Hazen, T.C., Andersen, G.L., 2013. Succession of hydrocarbon-degrading bacteria in the aftermath of the Deepwater Horizon oil spill in the gulf of Mexico. Environ. Sci. Technol. 47 (19), 10860–10867.

Edgar, R.C., 2013. UPARSE: highly accurate OTU sequences from microbial amplicon reads. Nat. Meth. 10 (10), 996–1000.

Enrique, L., Cédric, B., Hauke, H., Antonis, C., 2007. Cultivation-independent analysis reveals a shift in ciliate 18S rRNA gene diversity in a polycyclic aromatic hydrocarbon-polluted soil. FEMS Microbiol. Ecol. 62 (3), 365–373.

Friedman, J., Alm, E.J., 2012. Inferring correlation networks from genomic survey data. PLoS Comput. Biol. 8 (9) e1002687.

Gibson, J., Shokralla, S., Porter, T.M., King, I., van Konynenburg, S., Janzen, D.H., Hallwachs, W., Hajibabaei, M., 2014. Simultaneous assessment of the macro-biome and microbiome in a bulk sample of tropical arthropods through DNA metasystematics. Proc. Natl. Acad. Sci. U. S. A. 111 (22), 8007–8012.

Gieg, L.M., Fowler, S.J., Berdugo-Clavijo, C., 2014. Syntrophic biodegradation of hydrocarbon contaminants. Curr. Opin. Biotechnol. 27, 21–29.

Guillou, L., Bachar, D., Audic, S., Bass, D., Berney, C., Bittner, L., Boutte, C., Burgaud, G., de Vargas, C., Decelle, J., del Campo, J., Dolan, J.R., Dunthorn, M., Edvardsen, B., Holzmann, M., Kooistra, W.H.C.F., Lara, E., Le Bescot, N., Logares, R., Mahe, F., Massana, R., Montresor, M., Morard, R., Not, F., Pawlowski, J., Probert, I., Sauvadet, A.L., Siano, R., Stoeck, T., Vaulot, D., Zimmermann, P., Christen, R., 2013. The Protist Ribosomal Reference database (PR2): a catalog of unicellular eukaryote Small Sub-Unit rRNA sequences with curated taxonomy. Nucleic Acids Res. 41 (D1), 597–604.

Hawley, E.R., Piao, H., Scott, N.M., Malfatti, S., Pagani, I., Huntemann, M., Chen, A., Glavina del Rio, T., Foster, B., Copeland, A., Jansson, J., Pati, A., Tringe, S., Gilbert, J.A., Lorenson, T.D., Hess, M., 2014. Metagenomic analysis of microbial consortium from natural crude oil that seeps into the marine ecosystem offshore Southern California. Stand. Genom. Sci. 9 (3), 1259–1274.

Hong, S., Khim, J.S., Ryu, J., Park, J., Song, S.J., Kwon, B.O., Choi, K., Ji, K., Seo, J., Lee, S., Park, J., Lee, W., Choi, Y., Lee, K.T., Kim, C.K., Shim, W.J., Naile, J.E., Giesy, J.P., 2012. Two years after the Hebei Spirit oil spill: residual crude-derived hydrocarbons and potential AhR-mediated activities in coastal sediments. Environ. Sci. Technol. 46 (3), 1406–1414.

Hong, S., Khim, J.S., Ryu, J., Kang, S.G., Shim, W.J., Yim, U.H., 2014. Environmental and ecological effects and recoveries after five years of the Hebei Spirit oil spill, Taean, Korea. Ocean. Coast Manag. 102, 522–532.

Hong, S., Lee, S., Choi, K., Kim, G.B., Ha, S.Y., Kwon, B.O., Ryu, J., Yim, U.H., Shim, W.J., Jung, J., Giesy, J.P., Khim, J.S., 2015. Effect-directed analysis and mixture effects of AhR-active PAHs in crude oil and coastal sediments contaminated by the Hebei Spirit oil spill. Environ. Pollut. 199, 110–118.

Hong, S., Yim, U.H., Ha, S.Y., Shim, W.J., Jeon, S., Lee, S., Kim, C., Choi, K., Jung, J., Giesy, J.P., Khim, J.S., 2015. Bioaccessibility of AhR-active PAHs in sediments contaminated by the Hebei Spirit oil spill: application of Tenax extraction in effect-directed analysis. Chemosphere 144, 706–712.

Huson, D.H., Mitra, S., Ruscheweyh, H.J., Weber, N., Schuster, S.C., 2011. Integrative analysis of environmental sequences using MEGAN4. Genome Res. 21 (9), 1552–1560.

Il Lee, C., Kim, M.C., Kim, H.C., 2009. Temporal variation of chlorophyll a concentration in the coastal waters affected by the Hebei Spirit oil spill in the West Sea of Korea. Mar. Pollut. Bull. 58 (4), 496–502.

Jeong, H.J., Lee, H.J., Hong, S., Khim, J.S., Shim, W.J., Kim, G.B., 2015. DNA damage caused by organic extracts of contaminated sediment, crude, and weathered oil and their fractions recovered up to 5 years after the 2007 Hebei Spirit oil spill off Korea. Mar. Pollut. Bull. 95 (1), 452–457.

Ji, K., Seo, J., Liu, X., Lee, J., Lee, S., Lee, W., Park, J., Khim, J.S., Hong, S., Choi, Y., Shim, W.J., Takeda, S., Giesy, J.P., Choi, K., 2011. Genotoxicity and endocrine-disruption potentials of sediment near an oil spill site: two years after the Hebei Spirit oil spill. Environ. Sci. Technol. 45 (17), 7481–7488.

Jung, J.H., Chae, Y.S., Kim, H.N., Kim, M., Yim, U.H., Ha, S.Y., Han, G.M., An, J.G., Kim, E., Shim, W.J., 2012. Spatial variability of biochemical responses in resident fish after the M/V Hebei Spirit Oil Spill (Taean, Korea). Ocean. Sci. J. 47 (3), 209–214.

Kimes, N.E., Callaghan, A.V., Aktas, D.F., Smith, W.L., Sunner, J., Golding, B.T., Drzdowska, M., Hazen, T.C., Suflita, J.M., Morris, P.J., 2013. Metagenomic analysis and metabolite profiling of deep-sea sediments from the Gulf of Mexico following the Deepwater Horizon oil spill. Front. Microbiol. 4, 130–138.

King, G.M., Kostka, J.E., Hazen, T.C., Sobecky, P.A., 2015. Microbial responses to the Deepwater Horizon oil spill: from coastal wetlands to the Deep Sea. Annu. Rev. Mar. Sci. 7, 377–401.

Kleinsteuber, S., Schleinitz, K.M., Vogt, C., 2012. Key players and team play: anaerobic microbial communities in hydrocarbon-contaminated aquifers. Appl. Microbiol. Biotechnol. 94 (4), 851–873.

Kobayashi, Y., Hodoki, Y., Ohbayashi, K., Okuda, N., Nakano, S.-i., 2013. Grazing impact on the cyanobacterium Microcystis aeruginosa by the heterotrophic flagellate Collodictyon triciliatum in an experimental pond. Limnology 14 (1), 43–49.

Lozupone, C., Knight, R., 2005. UniFrac: a new phylogenetic method for comparing microbial communities. Appl. Environ. Microbiol. 71 (12), 8228–8235.

Maillard, J., Schumacher, W., Vazquez, F., Regeard, C., Hagen, W.R., Holliger, C., 2003. Characterization of the corrinoid iron-sulfur protein tetrachloroethene reductive dehalogenase of Dehalobacter restrictus. Appl. Environ. Microbiol. 69 (8), 4628–4638.

Mason, O.U., Scott, N.M., Gonzalez, A., Robbins-Pianka, A., Baelum, J., Kimbrel, J., Bouskill, N.J., Prestat, E., Borglin, S., Joyner, D.C., Fortney, J.L., Jurelevicius, D., Stringfellow, W.T., Alvarez-Cohen, L., Hazen, T.C., Knight, R., Gilbert, J.A., Jansson, J.K., 2014. Metagenomics reveals sediment microbial community response to Deepwater Horizon oil spill. Isme J. 8 (7), 1464–1475.

Massana, R., Gobet, A., Audic, S., Bass, D., Bittner, L., Boutte, C., Chambouvet, A., Christen, R., Claverie, J.-M., Decelle, J., Dolan, J.R., Dunthorn, M., Edvardsen, B., Forn, I., Forster, D., Guillou, L., Jaillon, O., Kooistra, W.H.C.F., Logares, R., Mahé, F., Not, F., Ogata, H., Pawlowski, J., Pernice, M.C., Probert, I., Romac, S., Richards, T., Santini, S., Shalchian-Tabrizi, K., Siano, R., Simon, N., Stoeck, T., Vaulot, D., Zingone, A., de Vargas, C., 2015. Marine protist diversity in European coastal waters and sediments as revealed by high-throughput sequencing. Environ. Microbiol. 17 (10), 4035–4049.

McCall, B.D., Pennings, S.C., 2012. Disturbance and recovery of salt marsh arthropod communities following BP Deepwater Horizon oil spill. PLoS One 7 (3), e32735.

Mendelssohn, I.A., Andersen, G.L., Baltz, D.M., Caffey, R.H., Carman, K.R., Fleeger, J.W., Joye, S.B., Lin, Q.X., Maltby, E., Overton, E.B., Rozas, L.P., 2012. Oil impacts on coastal wetlands: implications for the Mississippi River Delta ecosystem after the Deepwater Horizon oil spill. Bioscience 62 (6), 562–574.

Orphan, V.J., Taylor, L.T., Hafenbradl, D., Delong, E.F., 2000. Culture-dependent and culture-independent characterization of microbial assemblages associated with high-temperature petroleum reservoirs. Appl. Environ. Microbiol. 66 (2), 700–711.

Paul, J.H., Hollander, D., Coble, P., Daly, K.L., Murasko, S., English, D., Basso, J., Delaney, J., McDaniel, L., Kovach, C.W., 2013. Toxicity and mutagenicity of Gulf of Mexico waters during and after the Deepwater Horizon oil spill. Environ. Sci. Technol. 47 (17), 9651–9659.

Paulson, J.N., Stine, O.C., Bravo, H.C., Pop, M., 2013. Differential abundance analysis for microbial marker-gene surveys. Nat. Meth. 10 (12), 1200–1202.

Pennings, S.C., McCall, B.D., Hooper-Bui, L., 2014. Effects of oil spills on terrestrial arthropods in coastal wetlands. Bioscience 64 (9), 789–795.

Peterson, C.H., Rice, S.D., Short, J.W., Esler, D., Bodkin, J.L., Ballachey, B.E., Irons, D.B., 2003. Long-term ecosystem response to the Exxon Valdez oil spill. Science 302 (5653), 2082–2086.

Rivers, A.R., Sharma, S., Tringe, S.G., Martin, J., Joye, S.B., Moran, M.A., 2013. Transcriptional response of bathypelagic marine bacterioplankton to the Deepwater Horizon oil spill. Isme J. 7 (12), 2315–2329.

Rocke, E., Pachiadaki, M.G., Cobban, A., Kujawinski, E.B., Edgcomb, V.P., 2015. Protist community grazing on prokaryotic prey in deep ocean water masses. PLoS One 10 (4) e0124505.

Rodriguez, L.M., Overholt, W.A., Hagan, C., Huettel, M., Kostka, J.E., Konstantinidis, K.T., 2015. Microbial community successional patterns in beach sands impacted by the Deepwater Horizon oil spill. Isme J. 9 (9), 1928–1940.

Sagerup, K., Nahrgang, J., Frantzen, M., Larsen, L.-H., Geraudie, P., 2016. Biological effects of marine diesel oil exposure in red king crab (Paralithodes camtschaticus) assessed through a water and foodborne exposure experiment. Mar. Environ. Res. 119, 126–135.

Segata, N., Izard, J., Waldron, L., Gevers, D., Miropolsky, L., Garrett, W.S., Huttenhower, C., 2011. Metagenomic biomarker discovery and explanation. Genome Biol. 12 (6), 1–18.

Seo, J.-Y., Park, S.-H., Shin, H.-C., Lim, H.-S., Choi, J.-W., 2011. The early impacts of the 'Hebei Spirit' oil spill on the macrozoobenthic communities in the subtidal area around Tae-an, Western Coast of Korea. The Sea 16 (3), 139–146.

Shannon, P., Markiel, A., Ozier, O., Baliga, N.S., Wang, J.T., Ramage, D., Amin, N., Schwikowski, B., Ideker, T., 2003. Cytoscape: a software environment for integrated models of biomolecular interaction networks. Genome Res. 13 (11), 2498–2504.

Silliman, B.R., van de Koppel, J., McCoy, M.W., Diller, J., Kasozi, G.N., Earl, K., Adams, P.N., Zimmerman, A.R., 2012. Degradation and resilience in Louisiana salt marshes after the BP-Deepwater Horizon oil spill. Proc. Natl. Acad. Sci. U. S. A. 109 (28), 11234–11239.

Suarez-Suarez, A., Lopez-Lopez, A., Tovar-Sanchez, A., Yarza, P., Orfila, A., Terrados, J., Arnds, J., Marques, S., Niemann, H., Schmitt-Kopplin, P., Amann, R., Rossello-Mora, R., 2011. Response of sulfate-reducing bacteria to an artificial oil-spill in a coastal marine sediment. Environ. Microbiol. 13 (6), 1488–1499.

Thomsen, P., Willerslev, E., 2015. Environmental DNA – an emerging tool in conservation for monitoring past and present biodiversity. Biol. Conserv. 183, 4–18.

Turner, R.E., Overton, E.B., Meyer, B.M., Miles, M.S., Hooper-Bui, L., 2014. Changes in the concentration and relative abundance of alkanes and PAHs from the Deepwater Horizon oiling of coastal marshes. Mar. Pollut. Bull. 86 (1–2), 291–297.

van Gestel, C.A.M., van der Waarde, J.J., Derksen, J.G.M., van der Hoek, E.E., Veul, M.F.X.W., Bouwens, S., Rusch, B., Kronenburg, R., Stokman, G.N.M., 2001. The use of acute and chronic bioassays to determine the ecological risk and bioremediation efficiency of oil-polluted soils. Environ. Toxicol. Chem. 20 (7), 1438–1449.

Wang, Q., Garrity, G.M., Tiedje, J.M., Cole, J.R., 2007. Naïve bayesian classifier for rapid assignment of rRNA sequences into the new bacterial taxonomy. Appl. Environ. Microbiol. 73 (16), 5261–5267.

Xie, Y., Hong, S., Kim, S., Zhang, X., Yang, J., Giesy, J.P., Wang, T., Lu, Y., Yu, H., Khim, J.S., 2017. Ecogenomic responses of benthic communities under multiple stressors along the marine and adjacent riverine areas of northern Bohai Sea, China. Chemosphere 172, 166–174.

Yang, J., Zhang, X., Xie, Y., Song, C., Sun, J., Zhang, Y., Giesy, J.P., Yu, H., 2017. Ecogenomics of zooplankton community reveals ecological threshold of ammonia nitrogen. Environ. Sci. Technol.

Yim, U.H., Ha, S.Y., An, J.G., Won, J.H., Han, G.M., Hong, S.H., Kim, M., Jung, J.H., Shim, W.J., 2011. Fingerprint and weathering characteristics of stranded oils after the Hebei Spirit oil spill. J. Hazard. Mater. 197, 60–69.

eDNA-Based Bioassessment of Coastal Sediments Impacted by an Oil Spill

4   *Yuwei Xie[a], Xiaowei Zhang[a*], Jianghua Yang[a], Seonjin Kim[b], Seongjin Hong[c], John P.*

5   *Giesy[a,d,e,f], Un Hyuk Yim[g], Won Joon Shim[g], Hongxia Yu[a], Jong Seong Khim[b**]*

6   [a] State Key Laboratory of Pollution Control & Resource Reuse, School of the
7   Environment, Nanjing University, Nanjing, P. R. China, 210023

8   [b] School of Earth and Environmental Sciences & Research Institute of Oceanography,
9   Seoul National University, Seoul 08826, Republic of Korea

10   [c] Department of Ocean Environmental Sciences, Chungnam National University,
11   Daejeon 34134, Republic of Korea

12   [d] Department of Veterinary Biomedical Sciences and Toxicology Centre, University of
13   Saskatchewan, Saskatoon, Saskatchewan, Canada

14   [e] School of Biological Sciences, University of Hong Kong, Hong Kong, SAR, China

15   [f] Department of Biology, Hong Kong Baptist University, Hong Kong, SAR, China

16   [g] Oil and POPs Research Group, Korea Institute of Ocean Science and Technology

17   (KIOST), Geoje, Republic of Korea

18   **Corresponding Authors**

19   *   XWZ   phone: (+86)-25-83593649;   E-mail: zhangxw@nju.edu.cn,

20   howard50003250@yahoo.com

21   **JSK phone: (+82)-2-880-6750; E-mail: jskocean@snu.ac.kr

22 Supplementary figures

23 Figure S1. Shannon entropy rarefaction curves of bacterial (A), protistan (B) and

24 metazoan communities (C).

25 Figure S2. Tree plot of abundant phyla or supergroups.

26 Figure S3. Relative abundances of abundant classes of bacterial (A), protistan (B) and

27 metazoan communities (C) in sediments. Sediments were sorted by the concentration

28 of ΣPAHs. Only taxa with a mean relative abundance of ≥ 1% are shown.

29 Figure S4. Abundant components of micro- and macro-biota in sediments impacted

30 by the HSOS. Phylogenetic breakdown of the bacterial, protistan and metazoan data

31 set at the phylum level, eukaryotic supergroup and phylum level, respectively. (A)

32 Correlation between the structure of community or assemblage and the concentration

33 of ΣPAHs. (B) Correlation between the relative abundance of assemblage and the

34 concentration of ΣPAHs. (C) Correlation between the Shannon entropy of community

35 or assemblage and the concentration of ΣPAHs. Barcodes are "unclassified" when the

36 level of taxonomy could not reach that of phylum and were grouped as "others" when

37 relative abundance is smaller than 1%.

38

39 Supplementary tables

40 Table S1. Locations, sampling dates and chemical characteristics of sediments.

41 Table S2. Amount of sequences and alpha diversity in datasets. Biodiversity is

42 estimated by Shannon entropy for each sediment. Richness is measured by the

43   number of observed OTUs (OTU #).

44   Table S3. Pair-wise, post hoc comparisons between structures of communities and

45   dominant assemblages from different groups of ΣPAHs. Greater contamination level

46   (G); Lesser contamination (L); reference site (R). P values were calculated using the

47   9999 permutations procedure. Significant level of P value: ***, $P_{perm} < 0.001$; **,

48      $P_{perm} < 0.01$; *, $P_{perm} < 0.05$; ns: non-significant.

49

A

B

C

Gaemokhang.1
Gaemokhang.2
Gaemokhang.3
Naeri.1
Naeri.2
Naeri.3
Naeri.4
Sinduri.mf1
Sinduri.mf10
Sinduri.mf11
Sinduri.mf12
Sinduri.mf13
Sinduri.mf2
Sinduri.mf3
Sinduri.mf4
Sinduri.mf5
Sinduri.mf6
Sinduri.mf7
Sinduri.mf8
Sinduri.mf9
Sogeunri.mf1
Sogeunri.mf10
Sogeunri.mf2
Sogeunri.mf3
Sogeunri.mf4
Sogeunri.mf5
Sogeunri.mf6
Sogeunri.mf7
Sogeunri.mf8
Sogeunri.mf9

50
51   Figure S1.

52
53 Figure S2.

54

Legend (Panel A — Relative abundance of bacterial communities):
- *Acidimicrobiia*
- *Bacteroidia*
- *Flavobacteriia*
- *Anaerolineae*
- *Bacilli*
- *Clostridia*
- other bacterial classes
- *Planctomycetia*
- *α-proteobacteria*
- *δ-proteobacteria*
- *ε-proteobacteria*
- *γ-proteobacteria*
- *Verrucomicrobiae*

Legend (Panel B — Relative abundance of protistan communities):
- *Apusomonadidae*
- *Ascomycota*
- *Bacillariophyta*
- *Basidiomycota*
- *Breviatea*
- *Chlorophyceae*
- *Dinophyceae*
- *Endomyxa*
- *Filosa-Imbricatea*
- *Filosa-Thecofilosea*
- *MAST*
- other Apicomplexa classes
- other Fungi classes
- other protistan classes
- *Pirsonia*
- *Spirotrichea*
- *Trebouxiophyceae*
- *Ulvophyceae*

Legend (Panel C — Relative abundance of metazoan communities):
- *Actinopteri*
- *Arachnida*
- *Chromadorea*
- *Craniata*
- *Gastropoda*
- *Insecta*
- *Malacostraca*
- *Maxillopoda*
- other Arthropoda classes
- other metazoan classes
- *Polychaeta*

55

56   Figure S3.

57

58   Figure S4.

59   Table S1 was presented as a separated excel table.

Table S2. Amount of sequences and alpha diversity in datasets. Alpha diversity is estimated by Shannon entropy for each sediment. Richness is measured by the number of observed OTUs (OTU #).

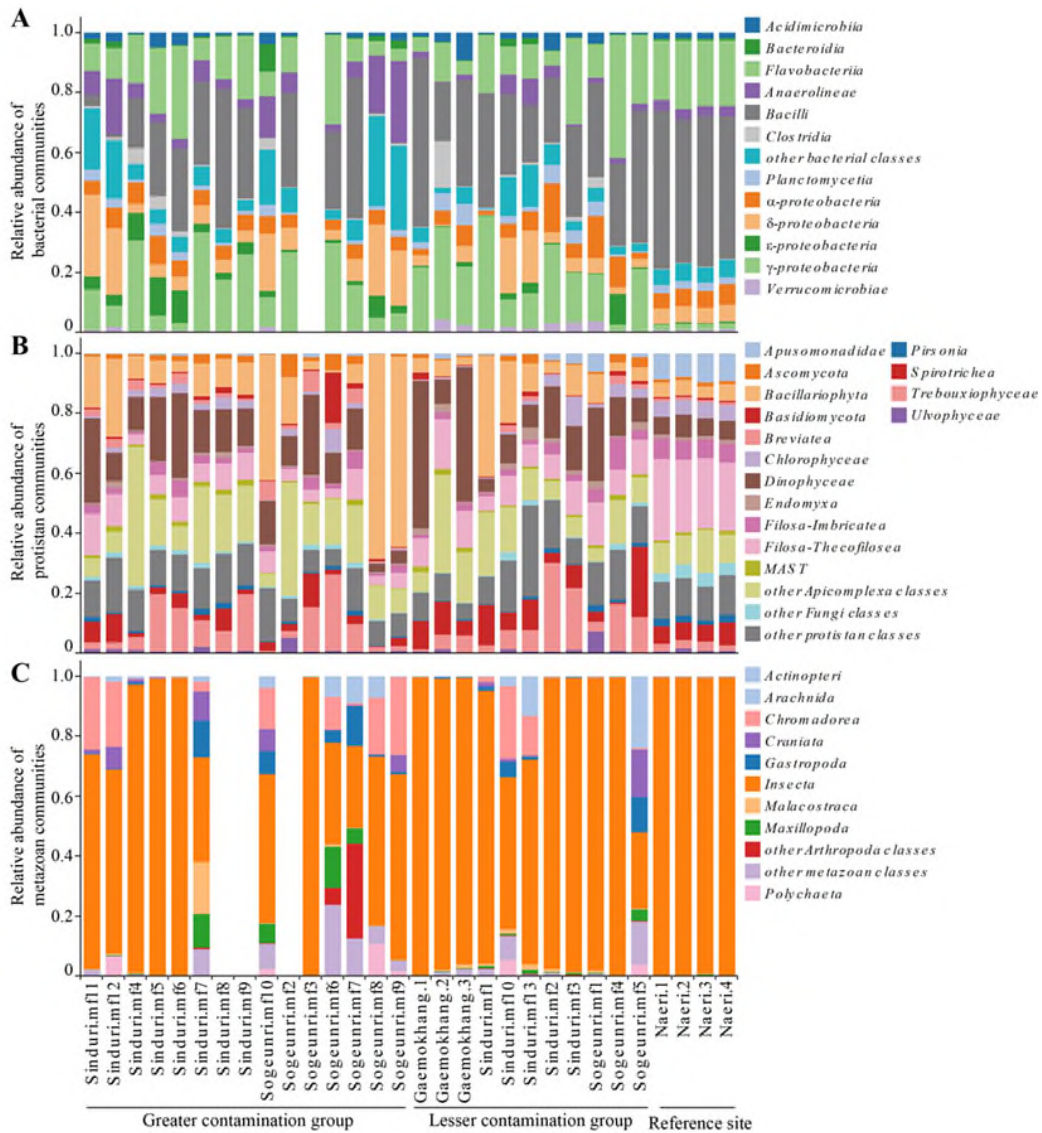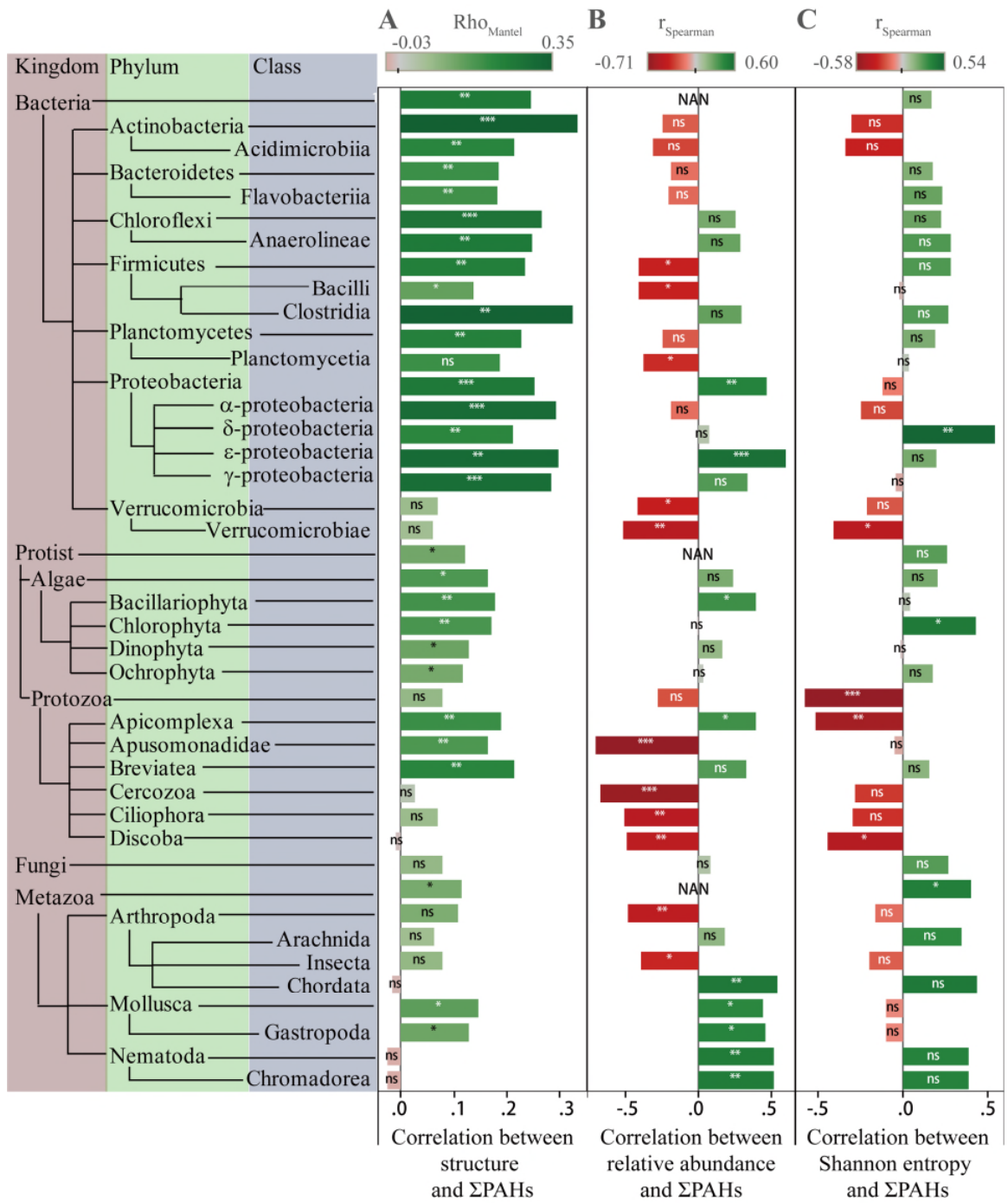| ID	16s rDNA V3				18s rDNA V9				COI			
	Reads		Alpha-diversity[a]		Reads		Alpha-diversity[a]		Reads		Alpha-diversity[a]	
	Sequenced	cleaned	OTU #[b]	SE[c]	Sequenced	cleaned	OTU #[b]	SE[c]	Sequenced	Cleaned[d]	OTU #[b]	SE[c]
Gaemokhang.1	77861	33294	1502.80	7.06	98812	25362	873.45	5.93	29126	15915	150.90	4.21
Gaemokhang.2	42262	28110	1389.70	7.20	77076	7982	964.00	7.06	56589	16627	161.00	4.58
Gaemokhang.3	51602	30999	2084.10	7.92	168740	41733	863.00	5.60	29964	14431	155.10	4.49
Naeri.1	48206	28583	2034.10	7.69	164228	18929	1065.45	6.82	24589	12476	174.75	4.95
Naeri.2	43649	24976	2040.90	7.88	75126	9126	1106.20	7.06	33967	12030	140.20	4.20
Naeri.3	51462	30783	1926.05	7.73	72333	8384	1048.60	6.75	38365	17895	131.30	4.17
Naeri.4	37365	21363	2038.00	7.94	143477	17088	1083.00	6.86	31365	13179	138.85	4.23
Sinduri.mf1	336298	295604	649.85	6.10	275557	78512	756.95	5.87	29376	11982	194.40	4.87
Sinduri.mf2	69392	38346	2245.85	9.19	64195	15872	928.80	7.21	57179	9554	188.40	5.93
Sinduri.mf3	36635	23187	1613.70	9.77	93866	25006	1014.15	6.75	26278	10595	165.90	4.82
Sinduri.mf4	308222	257922	1806.20	10.02	152868	63978	748.45	7.58	22286	10614	197.25	5.26
Sinduri.mf5	52248	30228	2093.65	9.30	68827	28024	1091.50	6.73	33534	19323	172.40	4.30
Sinduri.mf6	48607	27094	2083.95	8.10	113272	47313	1026.90	6.09	41428	20402	139.25	5.00
Sinduri.mf7	257463	216593	2312.60	7.35	151357	60060	770.15	6.20	8516	1220	65.00	4.77
Sinduri.mf8[e]	261809	227508	1997.05	7.53	233435	94129	711.20	7.25	15576			4.91
Sinduri.mf9[e]	297025	258411	1846.40	8.12	218015	73624	824.15	6.40	16814			4.80
Sinduri.mf10	160145	112323	3108.15	8.04	173393	43641	963.10	6.62	17820	4030	182.65	3.99
Sinduri.mf11	137846	106102	3591.45	8.07	188819	41987	823.75	6.83	18256	10790	133.50	4.70
Sinduri.mf12	280108	208016	3647.05	7.68	101291	16216	1099.85	7.43	19596	11656	152.80	
Sinduri.mf13	230576	181863	2933.90	7.55	193545	54796	554.65	6.91	11026	3440	110.45	

Sample												
Sogeunri.mf1	67168	39659	2092.75	7.91	78949	12158	1093.50	6.76	50600	13832	191.95	5.07
Sogeunri.mf2[e]	215694	176777	2208.90	10.29	171760	58844	415.90	6.67	7092			5.82
Sogeunri.mf3[f]	9920	3613		7.97	89409	30656	809.55	6.41	33548	14288	164.10	
Sogeunri.mf4	41643	25719	1472.65		162531	40255	928.95	5.88	51158	12482	149.30	4.68
Sogeunri.mf5	239553	208288	1383.85	7.06	133382	34843	583.05	6.85	15856	1422	44.85	4.27
Sogeunri.mf6	222127	195453	1494.00	6.84	125165	40945	235.70	6.68	13400	1220	55.00	4.27
Sogeunri.mf7	288774	230947	2291.95	7.16	139351	25868	726.50	4.87	25114	3520	118.70	4.43
Sogeunri.mf8	266297	153768	2993.85	8.11	210756	54194	719.45	7.05	15500	3522	166.00	5.29
Sogeunri.mf9	237574	141421	4069.00	9.22	100411	20648	854.40	6.88	28286	10592	157.75	5.48
Sogeunri.mf10	295171	173617	3935.40	10.53	90794	36734	907.85	7.01	30652	6988	202.05	5.32

[a] Alpha diversity was estimated by rarefaction twenty times to equal sequencing depth for relevant dataset (V3: 21,363; V9: 7,982; COI: 1,220).

[b] Number of observed OTUs

[c] Shannon entropy

[d] Metazoan OUTs (reads) were only extracted from the whole COI sequencing dataset

[e] Samples were discarded in metazoan community analyses, due to low sequencing depth

[f] One sample was discarded in bacterial community analyses, due to low sequencing depth

69   Table S3. Pair-wise, post hoc comparisons between structures of communities and dominant

70   assemblages from different groups of ΣPAHs. Greater contamination level (G); Lesser

71   contamination (L); reference site (R). P values were calculated using the 9999 permutations

72   procedure. Significant level of P value: ***, $P_{perm} < 0.001$; **, $P_{perm} < 0.01$; *, $P_{perm} <$

73   0.05; ns: non-significant.

74

Dataset	Dataset	T test
Bacteria	G vs L	2.05 ***
(n = 29)	G vs R	2.29 ***
	L vs R	1.50 *
Firmicutes	G vs L	2.06 **
	G vs R	2.26 ***
	L vs R	1.26 ns
Proteobacteria	G vs L	1.92 **
	G vs R	2.22 ***
	L vs R	1.36 *
Protist	G vs L	1.29 *
(n = 30)	G vs R	1.67 **
	L vs R	1.35 *
Algae	G vs L	1.34 *
	G vs R	1.66 **
	L vs R	1.26 *
Protozoa	G vs L	1.25 ns
	G vs R	1.62 **
	L vs R	1.25 ns
Metazoan	G vs L	1.38 ns
(n = 27)	G vs R	1.70 *
	L vs R	1.19 ns
Arthropoda	G vs L	1.42 ns
	G vs R	1.73 *
	L vs R	1.16 ns

75

Table S1. Locations, sampling dates and chemical characteristics of sediments.

ID	Location	Date	Latitude (°)	Longitude (°)	TOC (%)	Alkyl-PAHs [a] (ng/g dm)	Parent-PAHs [b] (ng/g dm)	ΣPAHs [c] (ng/g dm)	C2 phenanthrenes (ng/g dm)	C3 phenanthrenes (ng/g dm)	C2 dibenzothiophene (ng/g dm)	C3 dibenzothiophene (ng/g dm)
Gaemokhang.1	Gaemokhang	2007-12-13			1.01	491	13	505	46	39	82	79
Gaemokhang.2		2008-06-10	126.169	36.836	2.13	1921	59	1980	124	224	379	732
Gaemokhang.3		2008-10-14			0.54	335	41	376	38	56	15	31
Sinduri.mf1	Sinduri	2008-01-16	126.183	36.828	1.04	4595	87	4682	282	379	1100	1550
Sinduri.mf2		2008-10-14	126.183	36.828	0.79	32	19	51	3	4	ND[d]	ND
Sinduri.mf3		2009-06-19	126.183	36.828	1.61	85	39	123	9	11	5	13
Sinduri.mf4		2010-12-10	126.183	36.828	2.39	165771	3546	169317	8600	6900	29800	30600
Sinduri.mf5		2011-09-05	126.188	36.823	0.61	71002	1295	72297	3577	2927	11817	12587
Sinduri.mf6		2011-09-05	126.187	36.823	0.38	8998	101	9099	426	678	2040	3181
Sinduri.mf7		2012-01-11	126.187	36.823	1.80	63300	849	64149	3080	3380	15200	16900
Sinduri.mf8		2012-01-11	126.187	36.822	5.23	268551	2648	271199	12720	15641	66021	77622
Sinduri.mf9		2012-01-11	126.187	36.822	2.62	84763	887	85649	3667	5912	20607	30340
Sinduri.mf10		2013-09-09	126.187	36.823	1.50	44	11	54	3	3	6	9
Sinduri.mf11		2013-09-09	126.187	36.827	1.67	19263	411	19673	943	1948	2395	6077
Sinduri.mf12		2013-09-09	126.188	36.825	1.33	8114	176	8290	370	793	1280	2824
Sinduri.mf13		2013-09-09	126.186	36.821	1.37	47	5	52	2	4	7	12
Sogeunri.mf1	Sogeunri	2009-06-19	126.176	36.810	0.89	449	31	480	29	43	77	146
Sogeunri.mf2		2010-12-10	126.176	36.810	1.06	40936	1039	41975	1800	1290	5720	5750
Sogeunri.mf3		2011-09-05	126.171	36.819	0.89	8302	96	8397	381	413	1730	1982
Sogeunri.mf4		2011-09-05	126.171	36.819	1.68	2828	59	2886	154	145	524	667
Sogeunri.mf5		2012-01-11	126.171	36.818	1.03	1301	231	1532	89	124	66	100
Sogeunri.mf6		2012-01-11	126.171	36.819	0.50	16629	470	17099	1060	975	1670	2150
Sogeunri.mf7		2012-01-11	126.171	36.819	0.46	138095	1814	139909	7100	6760	29000	34700
Sogeunri.mf8		2014-10-28	126.186	36.814	0.40	192336	2951	195287	8264	16455	27713	72203
Sogeunri.mf9		2014-10-28	126.185	36.814	2.02	60433	1018	61451	2561	3733	5492	13739
Sogeunri.mf10		2014-10-28	126.184	36.813	0.89	36301	1333	37634	1477	3197	3882	8283
Naeri.1 - 4	Naeri[e]	2011-09-26	126.31	36.927	0.73	6	8	15	1	0	0	ND
				Min.	0.38	6	5	15	1	0	0	9
				Max.	5.23	268551	3546	271199	12720	16455	66021	77622
				Media	1.04	8650	204	8748	403	736	1730	3003
				Mean	1.35	45940	739	46679	2183	2769	9062	13425

	S.D.	0.97	69218	980	70123	3287	4369	15093	21189

[a] Alkyl-PAHs: sum of C1 naphthalene,C2 naphthalene,C3 naphthalene, C4 naphthalen, C1 fluorenes , C2 fluorenes, C3 fluorenes, C1 phenanthrenes, C2 phenanthrenes, C3 phenanthrenes, C4 ph

[b] Parent-PAHs: sum of naphthalene, acenaphthylene, fluorene, phenanthrene, dibenzothiophene, fluoranthene, benz[a]anthracene , chrysene, benzo[b]fluoranthene, benzo[k]fluoranthene, benzo[a]

[c] ΣPAHs: sum of alkyl- and parent-PAHs

[d] ND: not detected

[e] Naeri as refrence site

C3 chrysenes
(ng/g dm)
4
25
9
44
1
4
527
294
77
488
2217
930
1
629
209
1
9
108
48
20
34
157
974
1670
646
357
ND
1
2217
108
379

enanthrenes, C1 dibenzothiophene, C2 dibenzothiophene, C3 dibenzothiophene, C1 chrysenes, C2 chrysenes and C3 chrysenes

pyrene, indeno[1,2,3-cd]pyrene, dibenz[ah]anthracene and benzo[ghi]perylene